Long non-coding RNA FAM83H-AS1 induced by adipose-derived stem cells promotes breast and pancreatic cancer cell proliferation and migration

Jianing Tang
Wuhan University Zhongnan Hospital
Qiuxia Cui
Wuhan University Zhongnan Hospital
Dan Zhang
Huazhong University of Science and Technology
Xing Liao
Wuhan University Zhongnan Hospital
Yan Gong
Wuhan University Zhongnan Hospital
Gaosong Wu (wugaoson@163.com)
Wuhan University Zhongnan Hospital

Research

Keywords: FAM83H-AS1, adipose-derived stem cell, breast cancer, pancreatic cancer

Posted Date: April 24th, 2020

DOI: https://doi.org/10.21203/rs.3.rs-23457/v1

Abstract

Background

Stromal cells recruited to the tumor microenvironment and long non-coding RNAs (lncRNAs) in the tumor cells regulate cancer progression. However, their relationship is largely unknown.

Methods

In the current study, we identified the effects of lncRNA FAM83H-AS1, induced by adipose-derived stem cells (ADSCs) during tumor development, and explored the underlying mechanisms using a coculture cell model. Adipose tissues were obtained from healthy female donors, the expression of stromal markers on cell surface of expanded ADSCs were confirmed using immunofluorescence analysis. The breast and pancreatic cancer cells were cultured with or without ADSCs using 24-well transwell chamber systems with 8.0 μm pore size.

Results

Our results showed that FAM83H-AS1 was upregulated in breast and pancreatic cancers and associated with poor prognosis. ADSCs further induced FAM83H-AS1 and increased tumor cell proliferation via promoting G1/S transition through cyclin D1, CDK4 and CDK6. Wound healing, modified Boyden chamber and immunoblotting assays demonstrated that ADSCs induced epithelial-mesenchymal transition and migration of breast and pancreatic cancer cells in a FAM83H-AS1-dependent manner. And ADSC-induced FAM83H-AS1 increased unfolded protein response through AKT/XBP1 pathway.

Conclusion

In conclusion, our results indicated that ADSCs promoted breast and pancreatic cancer development via inducing cell proliferation and migration, as well as unfolded protein response through FAM83H-AS1.

Introduction

Long noncoding RNAs (lncRNA) are involved in cancer progression[1]. Their expression levels could be used as diagnostic or prognostic markers. Accumulating studies also confirmed the “seed and soil” relations between tumors and the surrounding microenvironment[2]. The tumor microenvironment consists of extracellular matrix and various mesenchymal cell types supported by a vascular network[3]. Tumor stromal is believed to exhibit many similarities in the inflammatory milieu produced by healing wounds, including angiogenesis, infiltration of fibroblasts and immune cells, and extensive remodeling of the extracellular matrix[4, 5].

As resident components of the tumor microenvironment, mesenchymal stem cells (MSCs) are recruited by the tumor cells and involved in the acceleration of cancer progression[6]. Upregulated cytokines and chemokines, such as IL-6, IL-1, TGF, CSF and SDF-1, induced MSC homing and MSC-derived factors, which in turn promoted cancer cell growth, migration, invasion, and/or distant metastasis[7–10]. Adipose-derived stem cells (ADSCs) are important components of MSCs and have the ability of adipogenic, chondrogenic, myogenic, osteogenic, cardiomyogenic and endothelial differentiation. Compared with bone marrow MSCs, ADSCs are more likely to be recruited, facilitating tumor vascularization, proliferation and malignancy[11, 12]. ADSCs secrete numerous important growth factors, cytokines, chemokines proangiogenic and inflammatory factors, including IGF, VEGF, IL-4, IL-6, IL-8, and IL-10[13–15]. Some studies reported that ADSC inhibited breast cancer growth and metastasis, and provoked prostate cancer cells apoptosis[16, 17]. However, the roles of ADSCs in tumor growth and progression are still controversial.

Endoplasmic reticulum (ER) functions as an essential synthesis and folding manufactory of secretory proteins. Hypoxia will cause the accumulation of misfolded protein in the ER, inducing ER stress. Unfolded protein response (UPR) is activated to clear misfolded proteins and restore normal physiological function[18, 19]. Human X-Box binding protein 1 (XBP1) was reported to efficiently induce UPR[20, 21]. Previous studies indicated that marrow fat cells induced ER stress in both tumor cells and the neighboring cells[22], And that XBP1 was induced in tumor cells cocultured with adipocyte, suggesting that ER stress in tumor cells was regulated by their microenvironment[23].

In the current study, we examined the role of ADSCs in cancer progression and explored the underlying mechanisms using a coculture cell system. Our data demonstrated that ADSCs enhanced lncRNA FAM83H-AS1 expression in cancer cells, and promoted cancer cells growth and migration via inducing UPR in a FAM83H-AS1-dependent manner.

Materials And Methods

Isolation and culture of human ADSCs

Adipose tissues were obtained from healthy female donors, aged 18 to 30 years, undergoing an abdominal liposuction bariatric procedure with written informed consent. This study was approved by the Ethics Committee for Human and Animal Research of Wuhan University. All experiments were performed in accordance with Declaration of Helsinki and other recognized standards. After washing with phosphate buffered saline (PBS), these lipoaspirates were finely minced and enzymatically digested with 2 mg/mL type I collagenase at 37 °C for 40 min. The tissues were then centrifuged to remove buoyant adipocytes. The top layers were retrieved to obtain the stromal vascular fractions (SVFs) and cultured in Dulbecco's modified eagle medium (DMEM, Hyclone, USA) F12 supplemented with 10% fetal bovine serum (FBS) and 1% antibiotic/antimycotic. ADSCs were obtained after 3-4 passages of SVFs cultured in the corresponding medium as reports[24].

Identification of ADSCs

The expression of stromal markers on cell surface of expanded ADSCs were confirmed using immunofluorescence analysis. ADSCs cultured on 14 mm slides in 24-well plates were fixed in 4% paraformaldehyde at room temperature for 30 minutes. After washing with PBS for 3 times, the cells were blocked with 10% goat serum and incubated with primary antibodies against CD31 (rat, Abcam, USA), CD45 (mouse, Santa Cruz, USA), CD90 (mouse, R&D, USA), and CD105 (rat, Santa Cruz, USA) at 4 °C overnight. After incubating with Alexa Fluor 488- and Cy3-conjugated secondary antibodies, 40,6-diamidino-2- phenylindole (DAPI, Sigma-Aldrich, USA) was used to stain the nuclei. The images were examined with a confocal microscope system (Nikon C2+ Confocal Microscope, Japan), and quantitatively evaluated using Image-Pro Plus 6.0 software to measure mean densities (IOD/area). For adipogenic differentiation, cells were seeded in 6-well plates. When full confluent, cells were cultured in DMEM/Ham's F12 media supplemented with 10μg/ml transferrin, 0.85 μM insulin, 0.2nM triiodothyronine, 1μM dexamethasone, 500μM isobutylmethylxanthine for 2 weeks. For osteogenic differentiation, cells were seeded in 6-well plates and maintained in DMEM/Ham's F12 media supplemented with 0.1mM dexamethasone, 50mM ascorbate-2-phosphate and 10mM b-glycerophosphate for 4 weeks.[25]. Differentiated ADSCs were stained with oil red for 30 minutes or alizarin for 30 minutes.

Culture and transfection of human tumor cells

The human breast cancer cells (MDA-MB-468) and pancreatic cancer cells (ASPC1, Procell, China) were maintained in DMEM supplemented with 10% FBS. All cells were cultured at 37 °C in a humidified 5% CO2 incubator. FAM83H-AS1 shRNAs (sh-1: 5'-GGACAGAGTAGGAGCGTAACT-3', sh-2: 5'-GCTGATTAGCAACCTTAGTTC-3', sh-3: 5'-GCAAAGCACTCCTTCTATCAG-3') were ligated into the Plko.1-Puro vector and packaged into lentiviruses (Viraltherapy, China). Lentiviral particles were used to infect the cancer cells to downregulate FAM83H-AS1 expression according to the manufacturer's instruction. To investigate the effects of ADSCs on cancer cell behaviors, ADSCs were cultured on the transwell inserts (Corning, USA) with 0.4 μm pore polycarbonate membranes, and cancer cells were cultured on the bottom chamber of the plates.

Proliferation, cell cycle and colony formation assay

The breast and pancreatic cancer cells were cultured with or without ADSCs for 3 days and then trypsinized. And they were seeded (2×10^3 cells/well) in 96-well plates and cultured in complete medium. Cell viability was measured using Cell Counting Kit-8 (CCK8) every 12 hours. Cancer cells were cultured with or without ADSCs for 48 hours. After washing with PBS for 3 times, the cells were stained with propidium iodide (Multisciences, China) and analyzed by flow cytometer (Beckman, USA). For the colony

formation assay, tumor cells were seeded (1-1.5×10^3 cells/well) in the bottom chamber of 6-well plates and maintained in complete medium for 2 weeks, ADSCs were cultured in the upper chamber. The cells were fixed with 4% paraformaldehyde for 2 hours, and stained with 1% crystal violet.

Xenograft tumor model

BALB/c nude mice aged 3 weeks were obtained from Beijing HFK Bioscience Co., Ltd. in Beijing, China. 1X106 MDA-MB-468/ASPC1 cells with or without 1X106 ADSCs were injected to each mouse. The mice were maintained in a temperature and humidity-controlled and specific pathogen-free environment in the laboratory animal facility of Zhongnan Hospital of Wuhan University. Tumor sizes were measured every 5 days until the end of the experiment. The experiments were performed under the protocols approved by ethnic committee of Zhongnan Hospital of Wuhan University.

Wound healing assay

The breast and pancreatic cancer cells were seeded in the bottom chamber of 6-well transwell plates with or without ADSCs cultured in the upper chamber. When full confluent, the cell layer was scratched with a 200 μl sterile pipette tip and washed with PBS. Images were acquired at different time points (0, 24, 48 h), and 3 independent experiments were conducted.

Modified Boyden chamber assay

The modified Boyden chamber assay was performed in 24-well transwell chamber systems (Corning, USA) with 8.0 μm pore size. The breast and pancreatic cancer cells were cultured with or without ADSCs for 3 days and then trypsinized. Cancer cells (5×10^4 cells/well) were seeded in the upper chamber insert and cultured in serum-free media. The lower chamber was filled with complete medium (600 μL, 10% FBS). After incubated at 37°C for 24 hours, the cells on the lower surface of the membrane were fixed with 4% paraformaldehyde and stained with crystal violet. The membranes were placed under an inverted phase contrast microscope and imaged to count the migrated cells. Three independent experiments were conducted.

Quantitative real-time polymerase chain reaction (qRT-PCR)

The total RNA was extracted from the cancer cells using the RNeasy Mini Kit (Qiagen, Germany). Reverse transcription was performed using the HiScript II 1st Strand cDNA Synthesis Kit (Vazyme, China). qRT-PCR was performed using the ChamQ SYBR qPCR Master Mix (Vazyme) with the CFX96TM Real-time PCR Detection System (Bio-Rad, USA). Relative expression was calculated using the $2^{-\Delta\Delta Ct}$ method,

which was normalized to glyceraldehyde 3-phosphate dehydrogenase (GAPDH). All assays were performed in triplicates. The primer sequences used for PCR are listed as follows. FAM83H-AS1 forward: 5'-TAGGAAACGAGCGAGCCC-3', and reverse: 5'-GCTTTGGGTCTCCCCTTCTT-3'; GAPDH forward: 5'-GGGAAACTGTGGCGTGAT-3', and reverse: 5'-GAGTGGGTGTCGCTGTTGA-3'.

Immunoblotting analysis

The breast and pancreatic cancer cells were lysed with RIPA extraction reagent (Beyotime, China) supplemented with protease and phosphatase inhibitors (Sigma-Aldrich, USA). Total protein was separated using 10-12.5% sodium dodecyl sulfate polyacrylamide gel electrophoresis and transferred to 0.45 μm PVDF membrane (Millipore, USA). Primary antibodies were E-cadherin, N-cadherin, Vimentin, cyclin D1, CDK4, CDK6, GAPDH (Proteintech, Chicago), p-IRE1, XBP1s (Abcam, UK), AKT, or p-AKT (Cell Signaling Technologies, USA) antibodies. Bands were visualized using an enhanced chemiluminescence (ECL) kit (Boster, China) and detected by ChemiDoc XRS+ Imaging System (Bio-Rad).

Statistical analysis

Student's t test and one-way ANOVA were used to compare 2 and more groups respectively. Multiple comparison with Bonferroni correction was performed when appropriate. A P value < 0.05 was considered as statistically significant and all tests were two-tailed. All statistical tests were performed with Prism 7.0 (GraphPad, USA).

Results

FAM83H-AS1 is up-regulated in breast cancer and pancreatic cancer samples and is associated with poorer prognosis

Using the web-based tool Gene Expression Profiling Interactive Analysis (GEPIA)[26], we found that lncRNA FAM83H-AS1 was upregulated in multiple tumors, including breast carcinoma, colon adenocarcinoma, lung cancer, pancreatic adenocarcinoma, prostate adenocarcinoma, rectum adenocarcinoma, stomach adenocarcinoma. The subsequent correlation assays indicated that the higher FAM83H-AS1 levels were only significantly correlated with worse prognosis in breast and pancreatic cancers (**Figure 1**).

ADSCs induce FAM83H-AS1 expression

Human ADSCs were isolated from human SVFs as previous reports[24, 25, 27]. Their morphology was fibroblast-like and spindle-like shape (**Figure 2A**). Immunofluorescence confirmed that they were CD90

and CD105 positive, while CD31 and CD45 negative (**Figure 2B**). The isolated ADSCs had the potential to differentiate into adipocytes and osteoblasts (**Figure 2C&D**). The ADSCs induced FAM83H-AS1 expression in the breast and pancreatic cancer cells (**Figure 3A&B, Figure S1A**).

ADSCs-induced FAM83H-AS1 promotes MDA-MA-468 and ASPC1 cell proliferation

Previous studies indicated that ADSCs promoted breast and pancreatic cancer development[27, 28]. To investigate whether FAM83H-AS1 was involved in the modulation of ADSCs on cancer growth, we downregulated FAM83H-AS1 in the breast and pancreatic cancer cells and examined cancer cell behaviors *in vitro*. All the 3 shRNAs significantly decreased FAM83H-AS1 expression (**Figure 3C, Figure S1B**), and shRNA-1 and shRNA-2 were selected for further analysis. The results of CCK-8 proliferation assays indicated that coculture with ADSCs increased cancer cell growth, and that deficiency of FAM83H-AS1 blocked ADSCs-induced proliferation (**Figure 3D, Figure S1C**). Colony formation assay suggested similar results. Compared with control group, the breast and pancreatic cancer cells cultured with ADSCs had significant higher colony formation number. FAM83H-AS1-knockdown significantly decreased colony formation of cancer cells (**Figure 3E, Figure S1D**). We investigated the role of ADSCs and FAM83H-AS1 in tumor growth by xenograft mice models. Our data showed that ADSCs-coculture significantly increased tumor growth and FAM83H-AS1 depletion by lentvirus based shRNA decelerated breast tumor growth (**Figure 3F**). These results revealed that FAM83H-AS1 was involved in ADSCs-induced breast and pancreatic tumor development via promoting cancer cell growth and proliferation.

ADSCs regulate cancer cell cycle G1-to-S transition via FAM83H-AS1

Flow cytometry analysis was used to investigate the effects of ADSCs and FAM83H-AS1 on cell cycle of breast and pancreatic cancer cells. Coculture with ADSCs significantly decreased the percentage of G1 cells but increased that of cells at the S phase, indicating that ADSCs promoted G1-to-S transition of cancer cells. However, deficiency of FAM83H-AS1 abrogated ADSC-induced G1-to-S phase transition. In addition, coculture with ADSCs increased the protein levels of cell cycle promoter cyclinD1, CDK4 and CDK6 in cancer cells, while knockdown of FAM83H-AS1 reversed ADSC-induced cell cycle protein upregulation (**Figure 4, Figure S2**).

ADSCs modulate cancer cell migration via FAM83H-AS1

To investigated the effects of ADSCs and FAM83H-AS1 on breast cancer and pancreatic cancer cell migration, MDA-MA-468 and ASPC1 cells were cocultured with ADCSs with or without FAM83H-AS1 knockdown, and applied for wound healing and modified Boyden chamber assays. The results showed that ADSC induced cancer cell migration, while deficiency of FAM83H-AS1 impeded this induction (**Figure**

5A&B, Figure S3A&B). ADSCs were reported to promote epithelial to mesenchymal transition (EMT) in cancer cells[29, 30]. The effects of FAM83H-AS1 on EMT of breast cancer and pancreatic cancer cells were further examined. Coculture with ADSCs resulted in a concurrent increase of N-cadherin, vimentin expression and a significant reduction of E-cadherin expression. FAM83H-AS1 knockdown reversed the effects of ADSCs on EMT markers (**Figure 5C, Figure S3C**). Taken together, these results indicated that FAM83H-AS1 modulated EMT and was involved in ADSCs-induced cell migration.

ADSCs induce the UPR and regulate XBP1/AKT pathway in a FAM83H-AS1-dependent manner

Bioinformatic analysis demonstrated that differentially expressed genes caused by FAM83H-AS1 knockdown were enriched in the UPR pathway[31]. The IRE1-XBP1 pathway was reported to activate the accumulation of unfolded/misfolded proteins in the ER. ER stress activated IRE1 and excised a 26 bp fragment from the mRNA encoding XBP1, thus initiating an essential UPR. To investigate whether ADSCs induced ER stress and regulated IRE1-XBP1 pathway, we examined the protein levels of IRE1 and XBP1 in cancer cells cocultured with ADSCs. In both MDA-MA-468 and ASPC1 cells, coculture with ADSCs upregulated IRE1 phosphorylation and XBP1 splicing, while deficiency of FAM83H-AS1 abrogated IRE1 phosphorylation and XBP1 splicing induced by ADSCs (**Figure 6A, Figure S4A**). Since previous studies revealed that AKT was regulated by FAM83H-AS1 and IRE1/XBP1, and ADSCs from primary breast cancer tissues promoted cancer cell proliferation via AKT pathway[14, 32-35], we hypothesized that FAM83H-AS1 modulated IRE1/XBP1/AKT pathway induced by ADSCs. Coculture with ADSCs activated AKT phosphorylation, while FAM83H-AS1 knockdown reversed this effect (**Figure 6A, Figure S4A**). In addition, IRE1 inhibitor STF-083010 downregulated XBP1s expression levels and AKT phosphorylation induced by ADSCs (**Figure 6B, Figure S4B**). Taken together, these results indicated that tumor progression regulated by ADSCs is modulated by FAM83H-AS1 via regulating AKT through XBP1s.

Metformin blocks ADSCs-induced cell proliferation

Discussion

Tumors are closely related and constantly interacted with their microenvironment. Increasing studies recognized that adipose tissue-derived cells, including cancer-related adipocytes and ADSCs, were recruited to tumor microenvironment and facilitate tumor growth[36–38]. Previous researched indicated that ADSCs enhanced cancer cell proliferation and migration in ovarian cancer, lung carcinoma, endometrial tumor, endometrial tumor, glioma and colon cancer[28–30, 39, 40]. Multiple cytokines and pathways were involved in the ADSC-induced tumor growth, such as IL-6, IL-1, TGF, CSF and SDF-1/CXCR4 signaling axis[7–10]. It was reported that ADSCs expressed and secreted IL-4, IL-8, IL-10, matrix metallopeptidase (MMP)-2, TGF, IGF, and VEGF, which enhanced anti-inflammatory reactions, potentially facilitating the growth and progression of breast tumor[13, 15].

In the present study, we isolated ADSCs from normal human adipose and investigated their roles in malignant biological behavior of breast and pancreatic cancer. We observed that lncRNA FAM83H-AS1 was upregulated in both breast and pancreatic cancer cells cocultured with ADSCs. Using the web-based tool GEPIA, we found that FAM83H-AS1 was upregulated in breast and pancreatic tumor tissues, and that elevated expression of FAM83H-AS1 was associated with poorer overall survival of breast and pancreatic cancer patients. Dysregulation of FAM83H-AS1 expression was also observed in colorectal carcinoma (CRC), and high FAM83HAS1 levels in CRC patients was significantly associated with advanced stage and poorer overall survival. Knockdown of FAM83H-AS1 dramatically inhibited the proliferation capability of CRC cells, and Notch 1 regulators reversed this effect mediated by FAM83H-AS1[41]. Analysis of 461 lung adenocarcinomas (LUAD) and 156 normal lung tissues revealed that FAM83H-AS1 was overexpressed in lung cancer and significantly associated with worse survival. FAM83H-AS1 was reported to enhance lung cancer ce3ll proliferation, migration and invasion via MET/EGFR signaling pathway[34]. In our analysis, coculture with ADSCs increased cancer cell proliferation and migration, while FAM83H-AS1 knockdown blocked ADSCs-induced proliferation and migration of breast and pancreatic cancer cells. In addition, deficiency of FAM83H-AS1 significantly caused G1 phase arrest. Expression levels of cell cycle promoter cyclin D1, CDK4 and CDK6 upregulated by ADSCs were abrogated by FAM83H-AS1 knockdown. Previous studies showed that deficiency of FAM83H-AS1 significantly caused the arrest of U251 and U87 cells at G1 phase and reduced protein levels of CDK2, CDK4 and CDK6 through recruiting EZH2 to the promoter of CDKN1A[42]. ADSCs were also reported to promote EMT of tumor cells[29, 30], we investigated whether ADSCs enhanced breast and pancreatic cancer cell migration through EMT. Cocultured with ADSCs resulted in a concurrent increase in N-cadherin, vimentin expression and a significant reduction in E-cadherin expression, while knockdown of FAM83H-AS1 reversed these ADSCs-induced effects. Taken together, these data indicated that FAM83H-AS1 regulated EMT and was involved in ADSCs-induced cell migration.

Gene set enrichment analysis of differentially expressed genes with FAM83H-AS1 knockdown in pancreatic cancer suggested that UNFOLDED PROTEIN RESPONSE, HYPOXIA, P53 PATHWAY, TNFA SIGNALING VIA NFKB and KRAS SIGNALING UP were the significantly enriched pathways[31]. In our analysis, ADSCs treatment significantly upregulated IRE1 phosphorylation and XBP1 splicing in cancer cells in a FAM83H-AS1-dependent manner. Previous studies revealed that AKT pathway was regulated by FAM83H-AS1 and IRE1/XBP1, ADSCs from primary breast cancer tissue promoted cancer cell proliferation via AKT[14, 32–35]. Our results demonstrated that coculture with ADSCs phosphorylated AKT, and that deficiency of FAM83H-AS1 decreased ADSCs-induced AKT phosphorylation. In addition, IRE1 inhibitor suppressed XBP1s, as well as AKT phosphorylation, induced by ADSCs. Taken together, our results indicated that tumor progression regulated by ADSCs was modulated by FAM83H-AS1 via regulating AKT through XBP1s.

Cancer cells and their surrounding microenvironment constantly communicate with each other during tumor development. In the present study, we found that ADSCs upregulated lncRNA FAM83H-AS1 expression in breast and pancreatic cancer cells, promoted cell proliferation and migration, and induced the unfolded protein response via activating IRE1-XBP1 pathway. FAM83H-AS1 was reported to

epidemically silence CDKN1A via recruiting EZH2 to its promoter and stabilize HuR protein via directly binding. The impact of ADSCs on tumor microenvironment and the direct mechanism of FAM83H-AS1 on IRE1-XBP1 pathway still need to be verified in further studies.

Conclusion

In conclusion, our present study demonstrated that ADSCs promoted breast and pancreatic cancer cell proliferation and migration, and induced the unfolded protein response in a FAM83H-AS1-dependent manner.

Declarations

Ethics approval and consent to participate

The research was carried out according to the World Medical Association Declaration of Helsinki and was approved by the Ethics Committee at Zhongnan Hospital of Wuhan University.

Consent for publication

Not applicable

Availability of data and materials

Not applicable

Competing interests

The authors have no conflicts of interest

Funding

None

Authors' contributions

YG and GW conceived and designed the study. JT, QC, DZ, and XL performed the experiments. JT and YG wrote the paper. GW reviewed and edited the manuscript. All authors read and approved the manuscript.

Acknowledgements

None

References

1. Rinn JL, Chang HY. Genome regulation by long noncoding RNAs. Annu Rev Biochem. 2012;81:145–66.
2. Hanahan D, Coussens LM. Accessories to the crime: functions of cells recruited to the tumor microenvironment. Cancer Cell. 2012;21:309–22.
3. Chaturvedi P, Gilkes DM, Wong CC, Luo W, Zhang H, Wei H, Takano N, Schito L, Levchenko A, Semenza GL. Hypoxia-inducible factor-dependent breast cancer-mesenchymal stem cell bidirectional signaling promotes metastasis. J Clin Invest. 2013;123:189–205.
4. Bussard KM, Mutkus L, Stumpf K, Gomez-Manzano C, Marini FC. Tumor-associated stromal cells as key contributors to the tumor microenvironment. Breast Cancer Res. 2016;18:84.
5. Dvorak HF. Tumors: wounds that do not heal. Similarities between tumor stroma generation and wound healing. N Engl J Med. 1986;315:1650–9.
6. Guan J, Chen J. Mesenchymal stem cells in the tumor microenvironment. Biomed Rep. 2013;1:517–21.
7. Rattigan Y, Hsu JM, Mishra PJ, Glod J, Banerjee D. Interleukin 6 mediated recruitment of mesenchymal stem cells to the hypoxic tumor milieu. Exp Cell Res. 2010;316:3417–24.
8. Tu S, Bhagat G, Cui G, Takaishi S, Kurt-Jones EA, Rickman B, Betz KS, Penz-Oesterreicher M, Bjorkdahl O, Fox JG, Wang TC. Overexpression of interleukin-1beta induces gastric inflammation and cancer and mobilizes myeloid-derived suppressor cells in mice. Cancer Cell. 2008;14:408–19.
9. Quante M, Tu SP, Tomita H, Gonda T, Wang SS, Takashi S, Baik GH, Shibata W, Diprete B, Betz KS, Friedman R, Varro A, Tycko B, et al. Bone marrow-derived myofibroblasts contribute to the mesenchymal stem cell niche and promote tumor growth. Cancer Cell. 2011;19:257–72.
10. Gao H, Priebe W, Glod J, Banerjee D. Activation of signal transducers and activators of transcription 3 and focal adhesion kinase by stromal cell-derived factor 1 is required for migration of human mesenchymal stem cells in response to tumor cell-conditioned medium. Stem Cells. 2009;27:857–65.
11. Zachar V, Rasmussen JG, Fink T. Isolation and growth of adipose tissue-derived stem cells. Methods Mol Biol. 2011;698:37–49.

12. Zhang Y, Daquinag AC, Amaya-Manzanares F, Sirin O, Tseng C, Kolonin MG. Stromal progenitor cells from endogenous adipose tissue contribute to pericytes and adipocytes that populate the tumor microenvironment. Cancer Res. 2012;72:5198–208.
13. Razmkhah M, Jaberipour M, Hosseini A, Safaei A, Khalatbari B, Ghaderi A. Expression profile of IL-8 and growth factors in breast cancer cells and adipose-derived stem cells (ASCs) isolated from breast carcinoma. Cell Immunol. 2010;265:80–5.
14. Xu L, Wang X, Wang J, Liu D, Wang Y, Huang Z, Tan H. Hypoxia-induced secretion of IL-10 from adipose-derived mesenchymal stem cell promotes growth and cancer stem cell properties of Burkitt lymphoma. Tumour Biol. 2016;37:7835–42.
15. Freese KE, Kokai L, Edwards RP, Philips BJ, Sheikh MA, Kelley J, Comerci J, Marra KG, Rubin JP, Linkov F. Adipose-derived stems cells and their role in human cancer development, growth, progression, and metastasis: a systematic review. Cancer Res. 2015;75:1161–8.
16. Sun B, Roh KH, Park JR, Lee SR, Park SB, Jung JW, Kang SK, Lee YS, Kang KS. Therapeutic potential of mesenchymal stromal cells in a mouse breast cancer metastasis model. Cytotherapy. 2009; 11: 289 – 98, 1 p following 98.
17. Takahara K, Ii M, Inamoto T, Komura K, Ibuki N, Minami K, Uehara H, Hirano H, Nomi H, Kiyama S, Asahi M, Azuma H. Adipose-derived stromal cells inhibit prostate cancer cell proliferation inducing apoptosis. Biochem Biophys Res Commun. 2014;446:1102–7.
18. Hetz C. The unfolded protein response: controlling cell fate decisions under ER stress and beyond. Nat Rev Mol Cell Biol. 2012;13:89–102.
19. Ron D, Walter P. Signal integration in the endoplasmic reticulum unfolded protein response. Nat Rev Mol Cell Biol. 2007;8:519–29.
20. Han D, Lerner AG, Vande Walle L, Upton JP, Xu W, Hagen A, Backes BJ, Oakes SA, Papa FR. IRE1alpha kinase activation modes control alternate endoribonuclease outputs to determine divergent cell fates. Cell. 2009;138:562–75.
21. Yoshida H, Matsui T, Yamamoto A, Okada T, Mori K. XBP1 mRNA is induced by ATF6 and spliced by IRE1 in response to ER stress to produce a highly active transcription factor. Cell. 2001;107:881–91.
22. Yuzefovych LV, Musiyenko SI, Wilson GL, Rachek LI. Mitochondrial DNA damage and dysfunction, and oxidative stress are associated with endoplasmic reticulum stress, protein degradation and apoptosis in high fat diet-induced insulin resistance mice. PLoS One. 2013;8:e54059.
23. Herroon MK, Rajagurubandara E, Diedrich JD, Heath EI, Podgorski I. Adipocyte-activated oxidative and ER stress pathways promote tumor survival in bone via upregulation of Heme Oxygenase 1 and Survivin. Sci Rep. 2018;8:40.
24. Zuk PA, Zhu M, Ashjian P, De Ugarte DA, Huang JI, Mizuno H, Alfonso ZC, Fraser JK, Benhaim P, Hedrick MH. Human adipose tissue is a source of multipotent stem cells. Mol Biol Cell. 2002;13:4279–95.
25. Yu X, Su B, Ge P, Wang Z, Li S, Huang B, Gong Y, Lin J. Human adipose derived stem cells induced cell apoptosis and s phase arrest in bladder tumor. Stem Cells Int. 2015; 2015: 619290.

26. Tang Z, Li C, Kang B, Gao G, Li C, Zhang Z. GEPIA: a web server for cancer and normal gene expression profiling and interactive analyses. Nucleic Acids Res. 2017;45:W98-w102.
27. Yan XL, Fu CJ, Chen L, Qin JH, Zeng Q, Yuan HF, Nan X, Chen HX, Zhou JN, Lin YL, Zhang XM, Yu CZ, Yue W, et al. Mesenchymal stem cells from primary breast cancer tissue promote cancer proliferation and enhance mammosphere formation partially via EGF/EGFR/Akt pathway. Breast Cancer Res Treat. 2012;132:153–64.
28. Ji SQ, Cao J, Zhang QY, Li YY, Yan YQ, Yu FX. Adipose tissue-derived stem cells promote pancreatic cancer cell proliferation and invasion. Braz J Med Biol Res. 2013;46:758–64.
29. Iser IC, Ceschini SM, Onzi GR, Bertoni AP, Lenz G, Wink MR. Conditioned Medium from Adipose-Derived Stem Cells (ADSCs) Promotes Epithelial-to-Mesenchymal-Like Transition (EMT-Like) in Glioma Cells In vitro. Mol Neurobiol. 2016;53:7184–99.
30. Chen D, Liu S, Ma H, Liang X, Ma H, Yan X, Yang B, Wei J, Liu X. Paracrine factors from adipose-mesenchymal stem cells enhance metastatic capacity through Wnt signaling pathway in a colon cancer cell co-culture model. Cancer Cell Int. 2015;15:42.
31. Arnes L, Liu Z, Wang J, Carlo Maurer H, Sagalovskiy I, Sanchez-Martin M, Bommakanti N, Garofalo DC, Balderes DA, Sussel L, Olive KP, Rabadan R. Comprehensive characterisation of compartment-specific long non-coding RNAs associated with pancreatic ductal adenocarcinoma. Gut. 2018.
32. Cunha DA, Gurzov EN, Naamane N, Ortis F, Cardozo AK, Bugliani M, Marchetti P, Eizirik DL, Cnop M. JunB protects beta-cells from lipotoxicity via the XBP1-AKT pathway. Cell Death Differ. 2014;21:1313–24.
33. Han CY, Lim SW, Koo JH, Kim W, Kim SG. PHLDA3 overexpression in hepatocytes by endoplasmic reticulum stress via IRE1-Xbp1s pathway expedites liver injury. Gut. 2016;65:1377–88.
34. Zhang J, Feng S, Su W, Bai S, Xiao L, Wang L, Thomas DG, Lin J, Reddy RM, Carrott PW, Lynch WR, Chang AC, Beer DG, et al. Overexpression of FAM83H-AS1 indicates poor patient survival and knockdown impairs cell proliferation and invasion via MET/EGFR signaling in lung cancer. Sci Rep. 2017;7:42819.
35. Cho JA, Park H, Lim EH, Kim KH, Choi JS, Lee JH, Shin JW, Lee KW. Exosomes from ovarian cancer cells induce adipose tissue-derived mesenchymal stem cells to acquire the physical and functional characteristics of tumor-supporting myofibroblasts. Gynecol Oncol. 2011;123:379–86.
36. Wozniak SE, Gee LL, Wachtel MS, Frezza EE. Adipose tissue: the new endocrine organ? A review article. Dig Dis Sci. 2009;54:1847–56.
37. Bonuccelli G, Avnet S, Grisendi G, Salerno M, Granchi D, Dominici M, Kusuzaki K, Baldini N. Role of mesenchymal stem cells in osteosarcoma and metabolic reprogramming of tumor cells. Oncotarget. 2014;5:7575–88.
38. Wang Y, Chu Y, Yue B, Ma X, Zhang G, Xiang H, Liu Y, Wang T, Wu X, Chen B. Adipose-derived mesenchymal stem cells promote osteosarcoma proliferation and metastasis by activating the STAT3 pathway. Oncotarget. 2017;8:23803–16.

39. Lu JH, Wei HJ, Peng BY, Chou HH, Chen WH, Liu HY, Deng WP. Adipose-Derived Stem Cells Enhance Cancer Stem Cell Property and Tumor Formation Capacity in Lewis Lung Carcinoma Cells Through an Interleukin-6 Paracrine Circuit. Stem Cells Dev. 2016;25:1833–42.
40. Klopp AH, Zhang Y, Solley T, Amaya-Manzanares F, Marini F, Andreeff M, Debeb B, Woodward W, Schmandt R, Broaddus R, Lu K, Kolonin MG. Omental adipose tissue-derived stromal cells promote vascularization and growth of endometrial tumors. Clin Cancer Res. 2012;18:771–82.
41. Lu S, Dong W, Zhao P, Liu Z. lncRNA FAM83H-AS1 is associated with the prognosis of colorectal carcinoma and promotes cell proliferation by targeting the Notch signaling pathway. Oncol Lett. 2018;15:1861–8.
42. Bi YY, Shen G, Quan Y, Jiang W, Xu F. Long noncoding RNA FAM83H-AS1 exerts an oncogenic role in glioma through epigenetically silencing CDKN1A (p21). J Cell Physiol. 2018;233:8896–907.

Supplementary Legends

Figure S1. The effect of ADSCs on FAM83H-AS1 and growth of human breast and pancreatic cancer cells. (A). ADSCs promoted FAM83H-AS1 expression in BXPC-3 and MDA-MB-231 cells. (B). shRNAs downregulated FAM83H-AS1 expression levels in BXPC-3 and MDA-MB-231 cells. (C). Growth curves of BXPC-3 and MDA-MB-231 cells determined via CCK-8 assays. (D). Colony formation assay of BXPC-3 and MDA-MB-231 cells. **, P < 0.01 by Student's t-test or one-way ANOVA with Bonferroni correction.

Figure S2. ADSCs promoted cell-cycle G1-to-S transition via FAM83H-AS1. (A). Flow cytometric analysis of BXPC-3 and MDA-MB-231 cells. (B). Immunoblotting of cyclin D1, CDK4 and CDK6 expression in BXPC-3 and MDA-MB-231 cells. The data were represented as the mean ± S.D. of 3 independent experiments. **, P < 0.01 by Student's t-test or one-way ANOVA with Bonferroni correction.

Figure S3. ADSCs promoted cancer cell migration via FAM83H-AS1. (A). Wound healing assay of BXPC-3 and MDA-MB-231 cells treated with or without FAM83H-AS1 shRNAs. (B). Modified Boyden chamber assay of BXPC-3 and MDA-MB-231 cells. (C) Immunoblotting of E-cadherin, N-cadherin and Vimentin expression in BXPC-3 and MDA-MB-231 cells. The data were represented as the mean ± S.D. of 3 independent experiments. **, P < 0.01 by Student's t-test or one-way ANOVA with Bonferroni correction.

Figure S4. ADSCs induced the unfolded protein response and regulated XBP1/AKT pathway in a FAM83H-AS1-dependent manner. (A). Immunoblotting of p-IRE1, XBP1s, AKT and p-AKT levels in BXPC-3 and MDA-MB-231 cells treated with or without FAM83H-AS1 shRNAs. (B). Immunoblotting of XBP1s, AKT and p-AKT levels in BXPC-3 and MDA-MB-231 cells cocultured with or without ADSCs and treated with or without IRE1 inhibitor STF-083010.

Figures

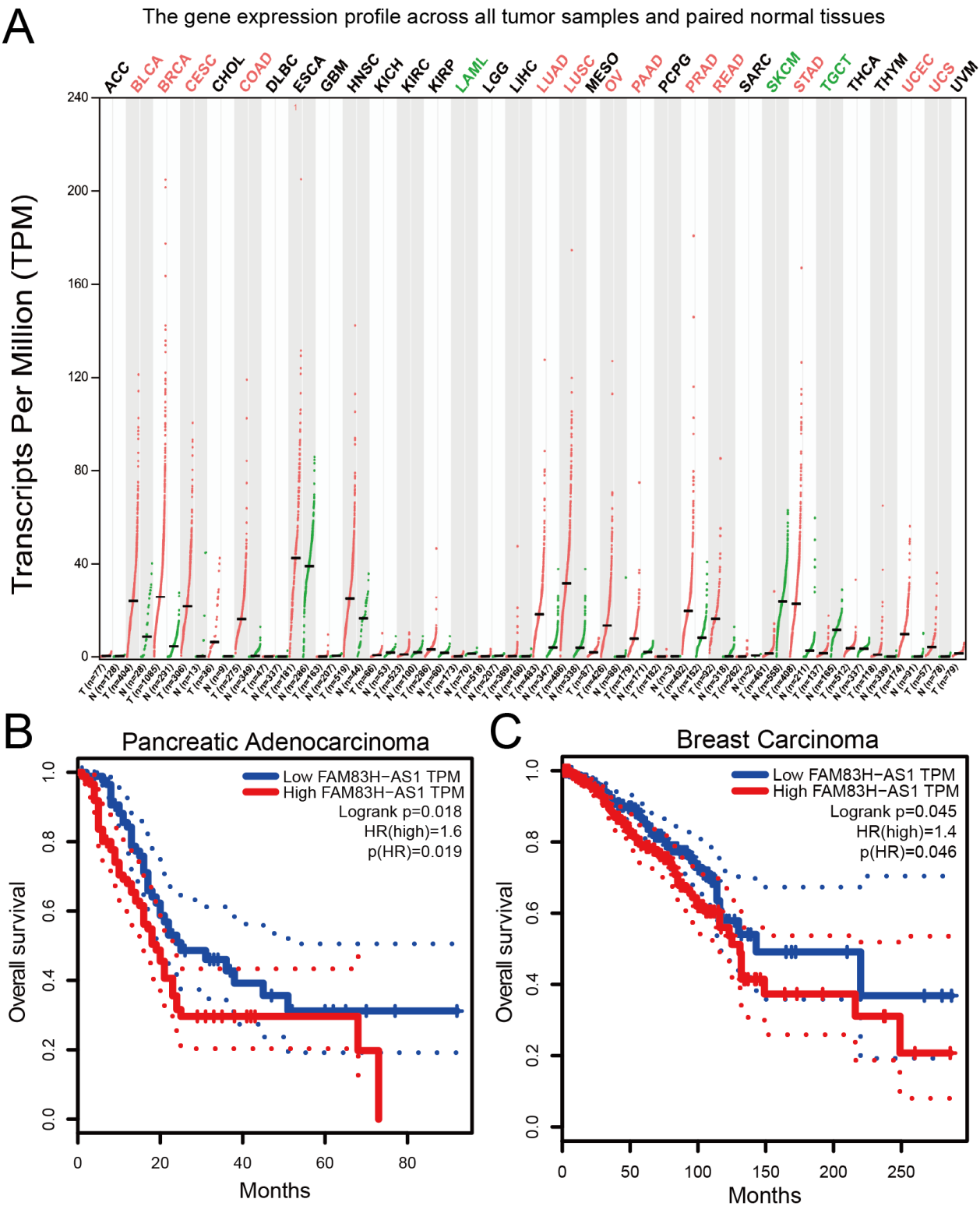

Figure 1

LncRNA FAM83H-AS1 expression. (A). The gene expression profile across all tumor samples and paired normal tissues. (B) Survival analysis of FAM83H-AS1 in pancreatic adenocarcinoma. (C). Survival analysis of FAM83H-AS1 in breast carcinoma.

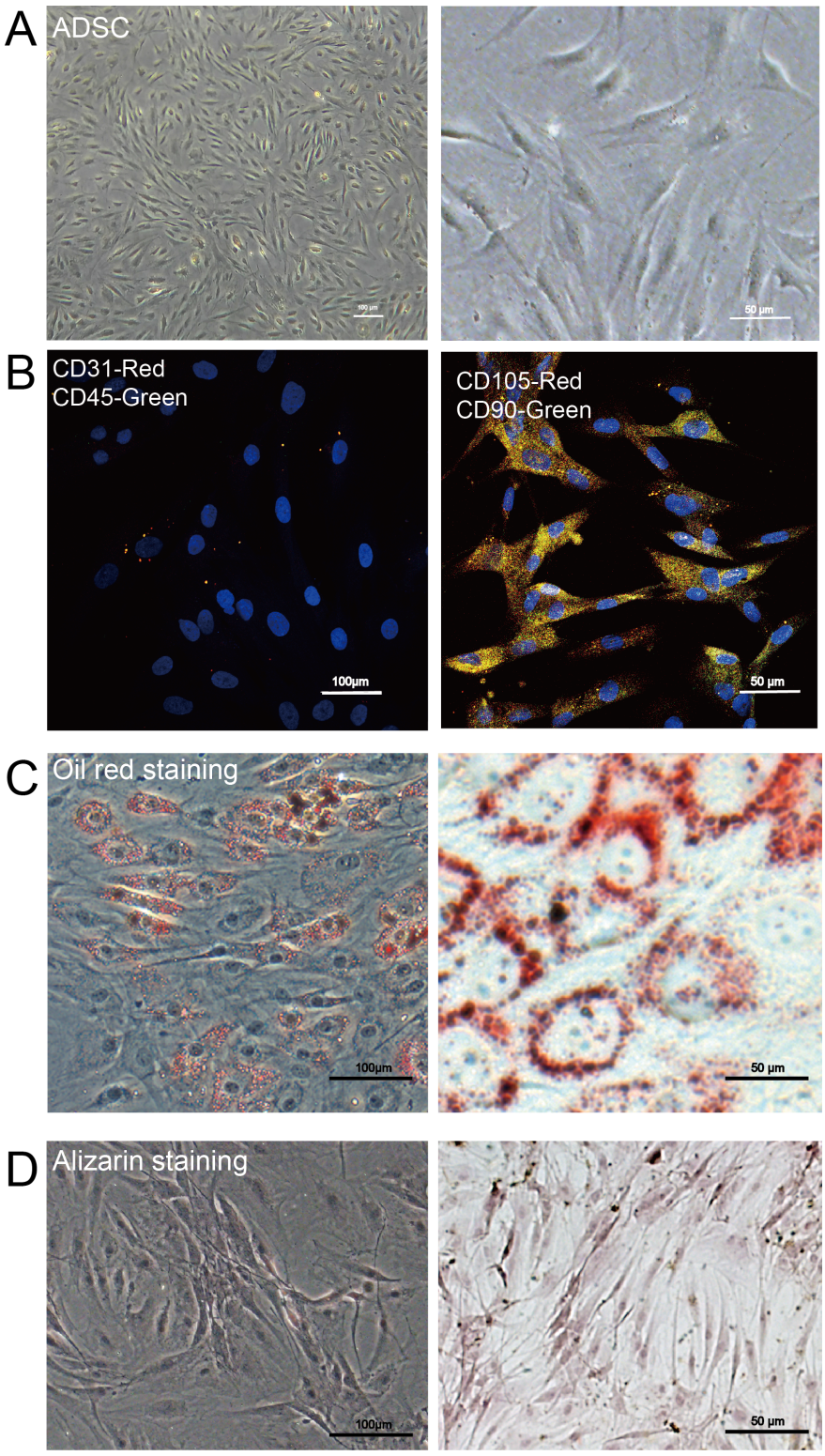

Figure 2

Identification of adipose-derived stem cells. (A). ADSCs had fibroblast-like and spindle-like morphology. (B). Representative immunofluorescent staining of CD31, CD45, CD90 and CD105. (C). Representative Oil Red O staining of adipogenesis. (D). Representative Alizarin Red S staining of osteogenesis.

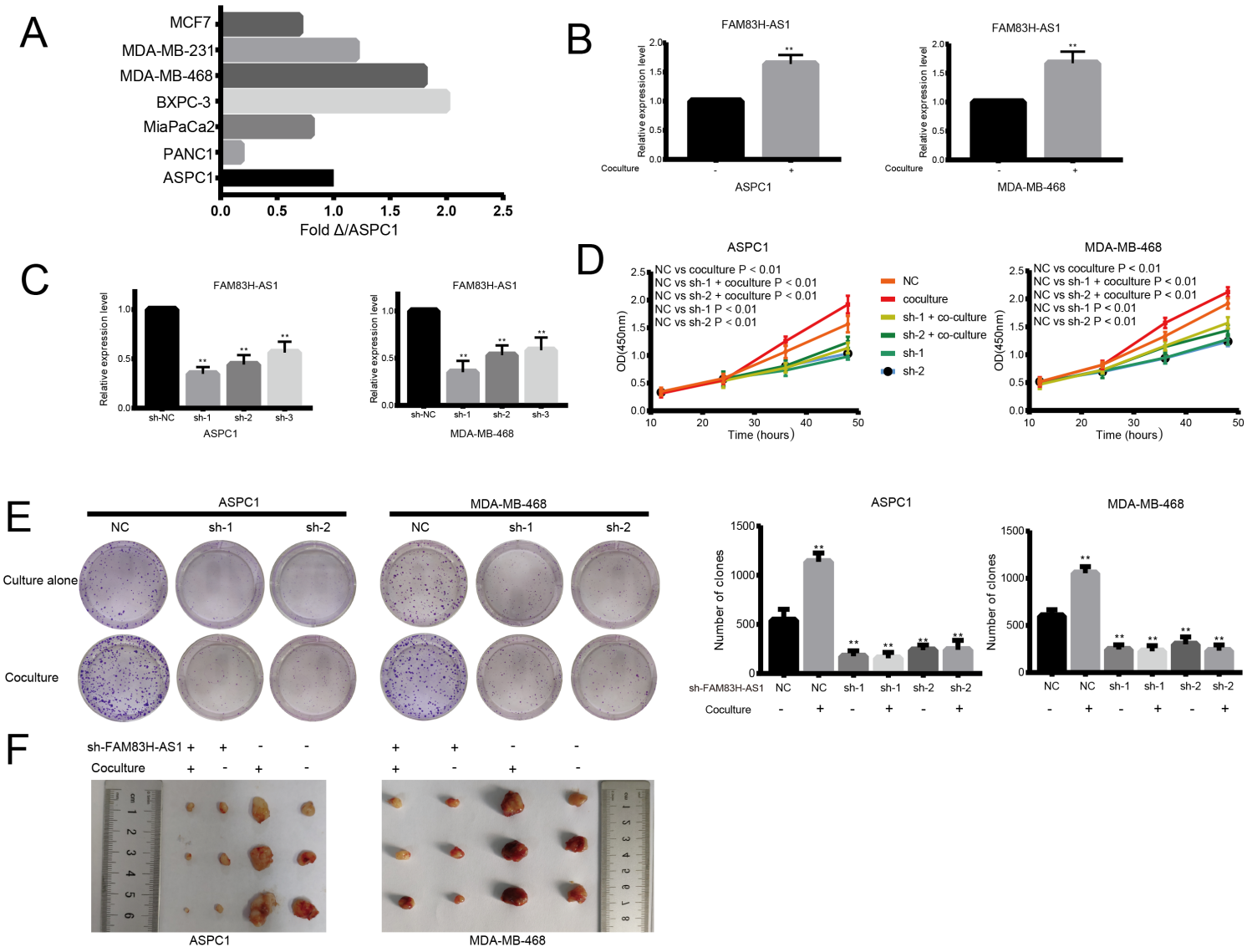

Figure 3

The effect of ADSCs on FAM83H-AS1 and growth of human breast and pancreatic cancer cells. (A). FAM83H-AS1 expression across a panel of cell lines relative to that in ASPC1. (B). ADSCs promoted FAM83H-AS1 expression in ASPC1 and MDA-MB-468 cells. (C). shRNAs downregulated FAM83H-AS1 expression levels in ASPC and MDA-MB-469 cells. (D). Growth curves of ASPC1 and MDA-MB-468 cells determined via CCK-8 assays. (E). Colony formation assay of ASPC1 and MDA-MB-468 cells.

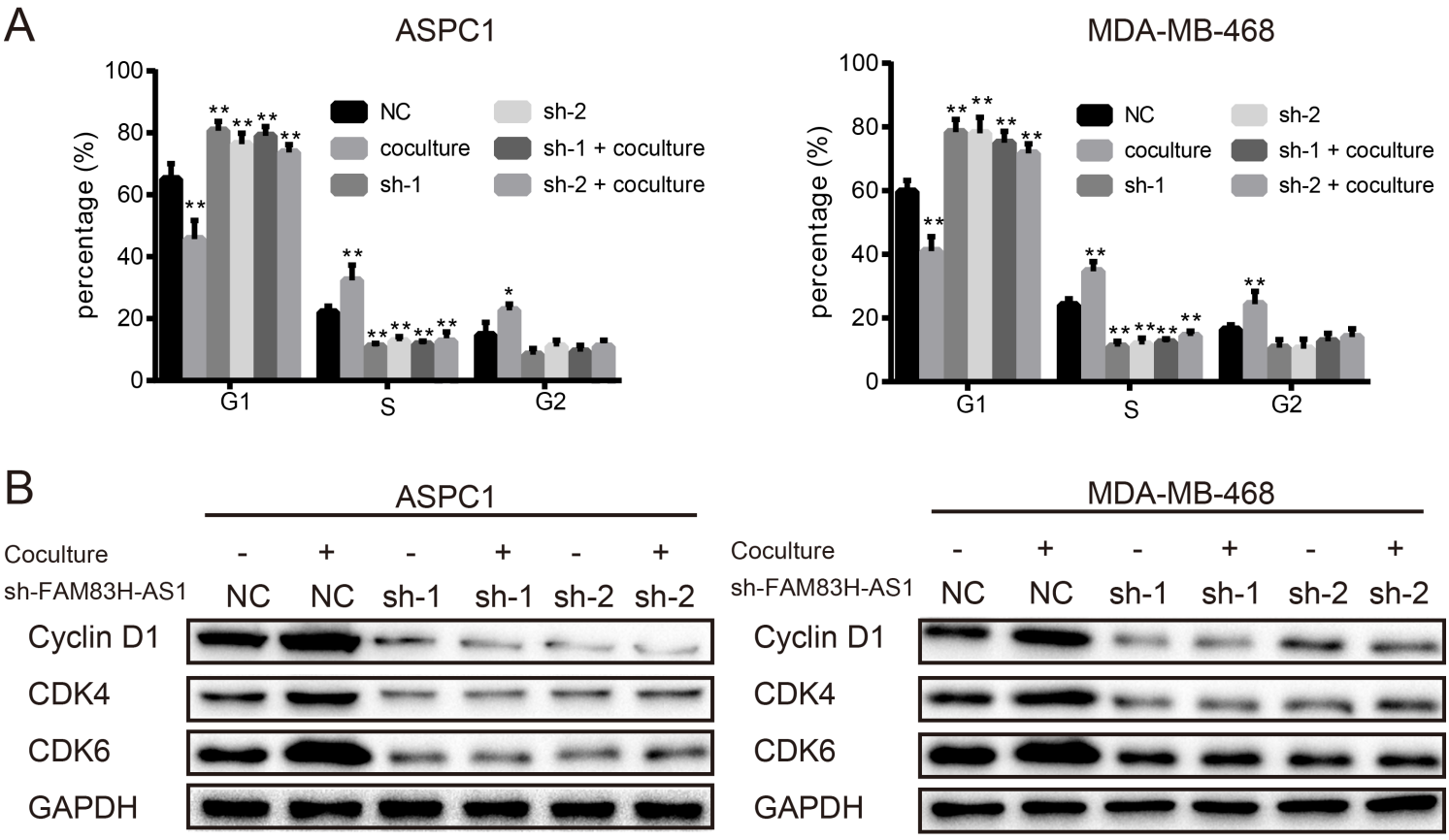

Figure 4

ADSCs promoted cell-cycle G1-to-S transition via FAM83H-AS1. (A). Flow cytometric analysis of ASPC1 and MDA-MB-468 cells. (B). Immunoblotting of cyclin D1, CDK4 and CDK6 expression in ASPC1 and MDA-MB-468 cells. The data were represented as the mean ± S.D. of 3 independent experiments. *, $P < 0.05$; **, $P < 0.01$ by Student's t-test or one-way ANOVA with Bonferroni correction.

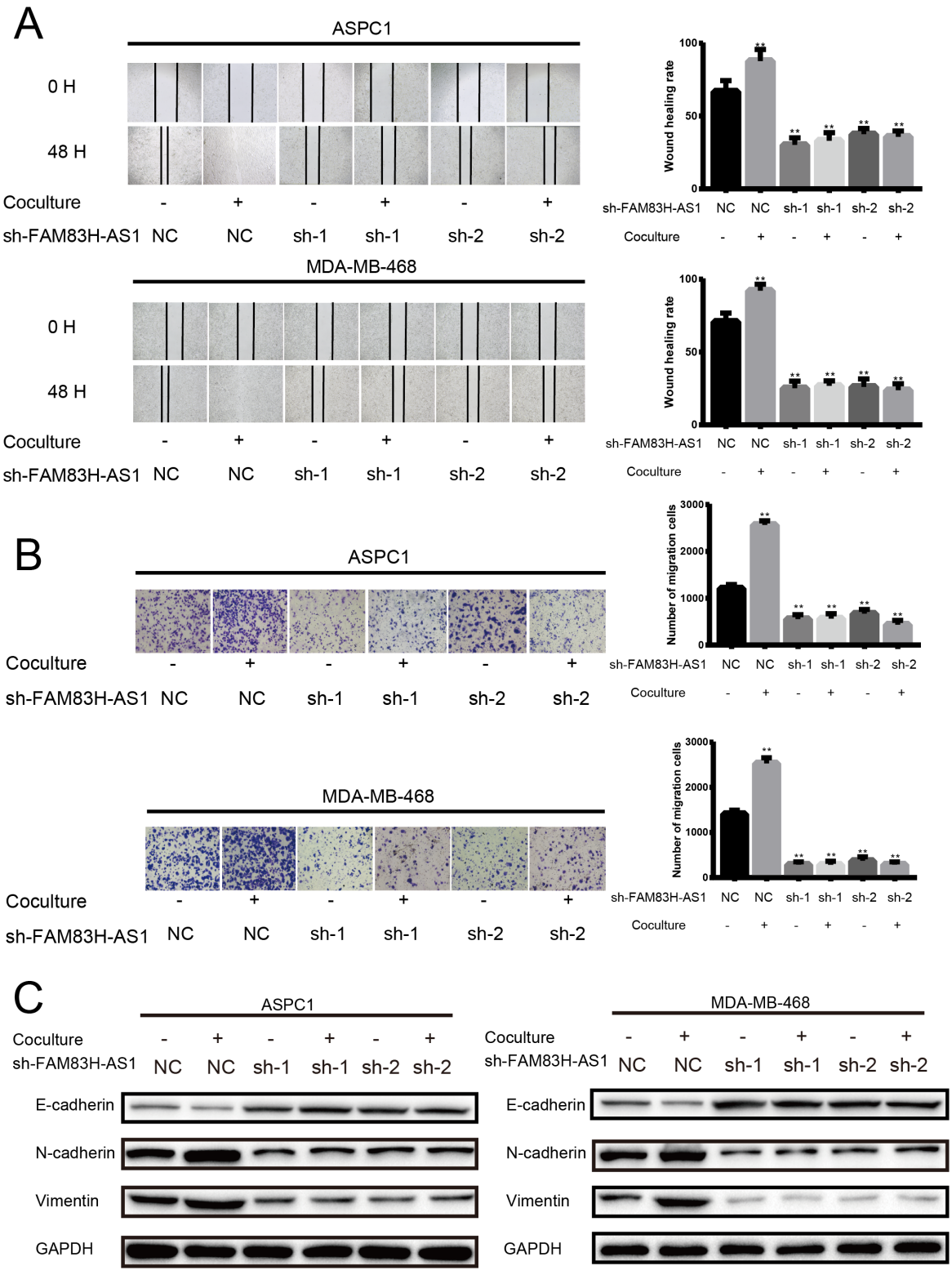

Figure 5

ADSCs promoted cancer cell migration via FAM83H-AS1. (A). Wound healing assay of ASPC1 and MDA-MD-468 cells. (B). Modified Boyden chamber assay of ASPC1 and MDA-MB-468 cells. (C). Immunoblotting of E-cadherin, N-cadherin and Vimentin expression in ASPC1 and MDA-MB-468 cells. The data were represented as the mean ± S.D. of 3 independent experiments. **, P < 0.01 by Student's t-test or one-way ANOVA with Bonferroni correction.

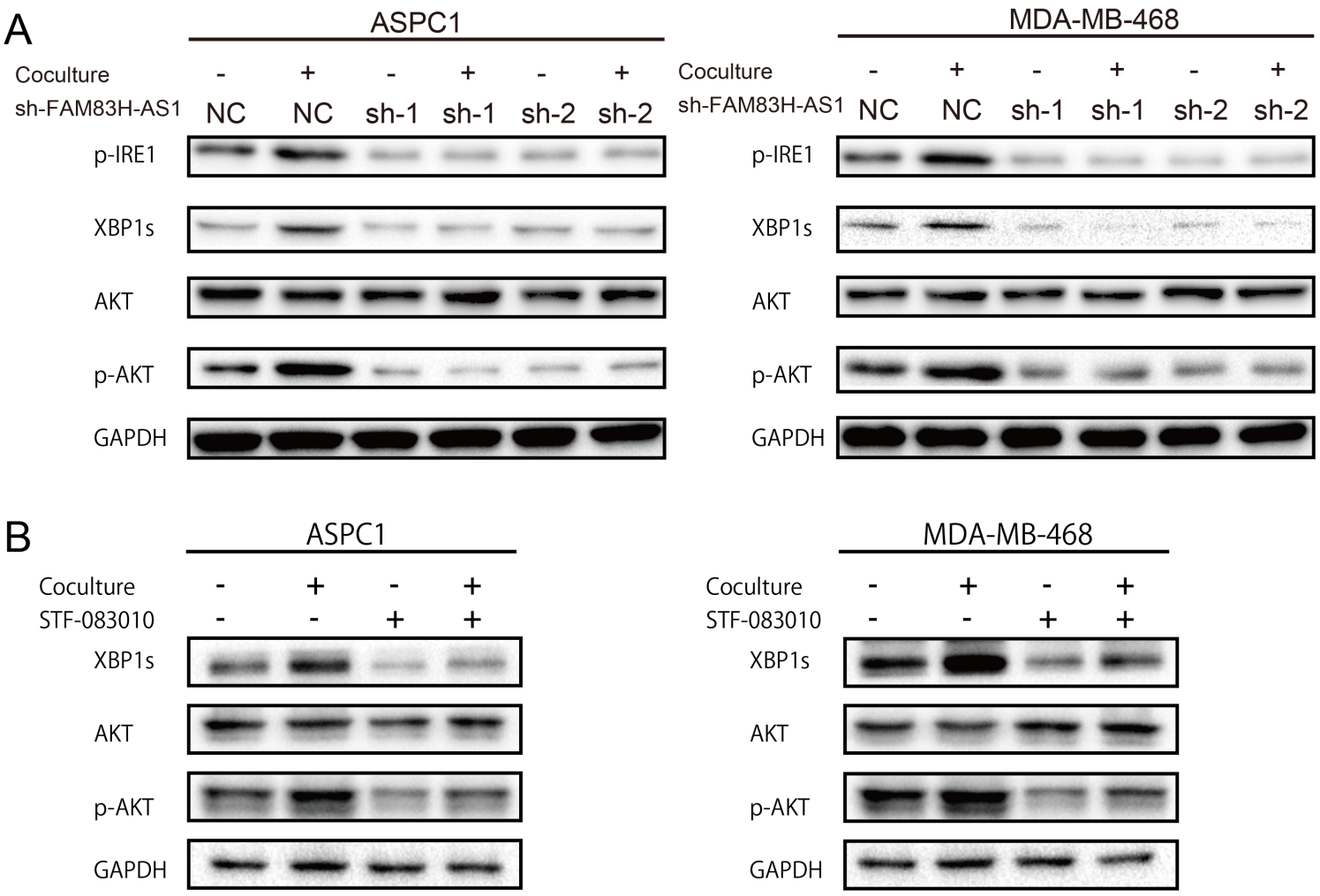

Figure 6

ADSCs induced the unfolded protein response and regulated XBP1/AKT pathway in a FAM83H-AS1-dependent manner. (A). Immunoblotting of p-IRE1, XBP1s, AKT and p-AKT protein levels in ASPC1 and MDA-MB-468 cells treated with or without FAM83H-AS1 shRNAs. (B). Immunoblotting of XBP1s, AKT and p-AKT expression in ASPC1 and MDA-MB-468 cells treated with or without IRE1 inhibitor STF-083010.

Supplementary Files

This is a list of supplementary files associated with this preprint. Click to download.

- FigureS2.tif
- FigureS1.tif
- FigureS3.tif
- FigureS4.tif